

AWARD NUMBER: W81XWH-18-1-0763

TITLE: Precision Targeting of Castration-Resistant Prostate Cancer with a Novel Ferrous Iron-Dependent Therapeutic Delivery and Tumor Imaging Strategy

PRINCIPAL INVESTIGATOR: Michael J. Evans

CONTRACTING ORGANIZATION: The Regents of the University of California, San Francisco
San Francisco, CA 94143-3110

REPORT DATE: OCTOBER 2019

TYPE OF REPORT: Annual

PREPARED FOR: U.S. Army Medical Research and Materiel Command
Fort Detrick, Maryland 21702-5012

DISTRIBUTION STATEMENT: Approved for Public Release; Distribution Unlimited

The views, opinions and/or findings contained in this report are those of the author(s) and should not be construed as an official Department of the Army position, policy or decision unless so designated by other documentation.

REPORT DOCUMENTATION PAGE

Form Approved
OMB No. 0704-0188

Public reporting burden for this collection of information is estimated to average 1 hour per response, including the time for reviewing instructions, searching existing data sources, gathering and maintaining the data needed, and completing and reviewing this collection of information. Send comments regarding this burden estimate or any other aspect of this collection of information, including suggestions for reducing this burden to Department of Defense, Washington Headquarters Services, Directorate for Information Operations and Reports (0704-0188), 1215 Jefferson Davis Highway, Suite 1204, Arlington, VA 22202-4302. Respondents should be aware that notwithstanding any other provision of law, no person shall be subject to any penalty for failing to comply with a collection of information if it does not display a currently valid OMB control number. **PLEASE DO NOT RETURN YOUR FORM TO THE ABOVE ADDRESS.**

1. REPORT DATE OCTOBER 2019		2. REPORT TYPE ANNUAL		3. DATES COVERED 30SEP2018 - 29SEP2019	
4. TITLE AND SUBTITLE: Precision Targeting of Castration-Resistant Prostate Cancer with a Novel Ferrous Iron-Dependent Therapeutic Delivery and Tumor Imaging Strategy				5a. CONTRACT NUMBER W81XWH-18-1-0763	
				5b. GRANT NUMBER	
				5c. PROGRAM ELEMENT NUMBER	
6. AUTHOR(S) Michael J. Evans E-Mail: Michael.Evans@ucsf.edu				5d. PROJECT NUMBER	
				5e. TASK NUMBER	
				5f. WORK UNIT NUMBER	
7. PERFORMING ORGANIZATION NAME(S) AND ADDRESS(ES) The Regents of the University of California, San Francisco San Francisco, CA 94143-3110				8. PERFORMING ORGANIZATION REPORT NUMBER	
9. SPONSORING / MONITORING AGENCY NAME(S) AND ADDRESS(ES) U.S. Army Medical Research and Materiel Command Fort Detrick, Maryland 21702-5012				10. SPONSOR/MONITOR'S ACRONYM(S)	
				11. SPONSOR/MONITOR'S REPORT NUMBER(S)	
12. DISTRIBUTION / AVAILABILITY STATEMENT Approved for Public Release; Distribution Unlimited					
13. SUPPLEMENTARY NOTES					
14. ABSTRACT We propose that mechanistically unrelated anti-cancer therapeutics can be more effectively deployed by administration in a pro-drug form that conditionally releases the therapeutic after chemical reaction with Fe(II), pools of which are augmented in CRPC cells and in the tumor microenvironment. To test and validate our hypothesis we will synthesize and evaluate in multiple prostate cancer models three novel agents, the Fe(II)-activated form of a potent DNA-alkylator (TRX-CBI), the Fe(II)-activated form of enzalutamide (TRX-ENZ), and a novel Fe(II)-targeted therapeutic radionuclide, 117Lu-TRX. We will also image prostate cancer in diverse animal models using an Fe(II)-activated PET probe (18F-TRX). Our objective is to show that castration resistant prostate cancer can be addressed effectively with these novel Fe(II)-targeted approach and that response to therapy can be predicted with 18F-TRX. Successful realization of these objectives via the IDA mechanism will greatly enable our long-term goal of identifying a "theranostic" development candidate that can be progressed toward first-in-human studies.					
15. SUBJECT TERMS NONE LISTED					
16. SECURITY CLASSIFICATION OF:			17. LIMITATION OF ABSTRACT	18. NUMBER OF PAGES	19a. NAME OF RESPONSIBLE PERSON
a. REPORT	b. ABSTRACT	c. THIS PAGE			USAMRMC
Unclassified	Unclassified	Unclassified	Unclassified	17	19b. TELEPHONE NUMBER (include area code)

TABLE OF CONTENTS

	<u>Page</u>
1. Introduction	4
2. Keywords	4
3. Accomplishments	4 - 14
4. Impact	14
5. Changes/Problems	15
6. Products	16
7. Participants & Other Collaborating Organizations	16 - 17
8. Special Reporting Requirements	17
9. Appendices	17

1. INTRODUCTION:

We propose that mechanistically unrelated anti-cancer therapeutics can be more effectively deployed by administration in a pro-drug form that conditionally releases the therapeutic after chemical reaction with Fe(II), pools of which are augmented in CRPC cells and in the tumor microenvironment. To test and validate our hypothesis we will synthesize and evaluate in multiple prostate cancer models three novel agents, the Fe(II)-activated form of a potent DNA-alkylator (TRX-CBI), the Fe(II)-activated form of enzalutamide (TRX-ENZ), and a novel Fe(II)-targeted therapeutic radionuclide, ^{117}Lu -TRX. We will also image prostate cancer in diverse animal models using an Fe(II)-activated PET probe (^{18}F -TRX). Our objective is to show that castration resistant prostate cancer can be addressed effectively with these novel Fe(II)-targeted approach and that response to therapy can be predicted with ^{18}F -TRX. Successful realization of these objectives via the IDA mechanism will greatly enable our long-term goal of identifying a “theranostic” development candidate that can be progressed toward first-in-human studies.

2. **KEYWORDS:** Molecular imaging, cancer theranostics, pro-drug, iron metabolism, fluorine-18, lutetium-177, pharmacology, castration resistant prostate cancer

3. ACCOMPLISHMENTS:

What were the major goals of the project?

The major goal for project period one is listed below with the subtasks stipulated in the approved statement of work. An additional column, termed “status” has been added to indicate whether, or to what extent, the subtask has been completed. Where appropriate, specific dates have been added to indicate when the subtask was completed.

Specific Aim 1(specified in proposal)	Timeline	Site 1	Site 2	Site 3	Status
Major Task 1: In vivo evaluation of ¹⁸F-TRX	Months				
Subtask 1: Synthesis of ¹⁸ F-TRX and ¹⁸ F-DXL	1-2	Dr. Renslo	Dr. Evans		Completed, Dec. 2018
Subtask 2: Breeding the colony of genetically engineered mice for imaging with ¹⁸ F-TRX and treatment with TRX-CBI	1-14			Dr. Ruggero (50 mice)	Ongoing
Subtask 3: PET and biodistribution studies in nu/nu mice bearing PC3 tumors with ¹⁸ F-TRX and ¹⁸ F-DXL Cell lines: PC3 (ATCC)	3-4		Dr. Evans (40 mice)		Completed, Feb. 2019
Subtask 4: PET and biodistribution studies of ¹⁸ F-TRX in mice bearing xenografts: LNCaP-AR, PC3 and tumor sublines with stable MYC knockdown Cell lines: LNCaP-AR (Sawyers, MSKCC)	4-6		Dr. Evans (20 mice)		Ongoing, 50% completed
Subtask 5: PET and biodistribution studies of ¹⁸ F-TRX in mice bearing xenografts: DU145, LAPC4, and tumor sublines with stable PTEN knockdown Cell lines: DU145 (ATCC), LAPC4 (UCLA)	6-10		Dr. Evans (20 mice)		Ongoing, 50% completed
Subtask 6: PET and biodistribution studies of ¹⁸ F-TRX in genetically engineered mouse models	10-14		Dr. Evans	Dr. Ruggero (18 mice)	Completed,
Milestone(s) Achieved: Determination of tumor uptake of ¹⁸ F-TRX in vivo	14	Dr. Renslo	Dr. Evans	Dr. Ruggero	
Local IRB/IACUC Approval	2		Dr. Evans	Dr. Ruggero	Completed, Dec. 2018
Milestone Achieved: ACURO Approval	2		Dr. Evans	Dr. Ruggero	Completed, Dec. 2018

What was accomplished under these goals?

1) Major activities:

The primary focus of the first project period was to synthesize and evaluate the biodistribution of a radiofluorinated 1,2,4-trioxolane molecule, termed ^{18}F -TRX. After completing the radiosynthesis, the ^{18}F -TRX was to be evaluated in a panel of prostate cancer models of increasing complexity and clinical relevance, from subcutaneous cell line implants, to genetically engineered mouse models with mutations expected to alter the intracellular labile iron pool (LIP). The scientific purpose of these studies was to establish that (1) mouse models of prostate cancer have an elevated LIP, (2) the LIP concentration is sufficiently high to retain measurable concentration of an imaging avatar for a TRX therapeutic (i.e. ^{18}F -TRX), and (3) to determine site(s) of normal tissue uptake that could represent sources of toxicity for a cognate TRX therapeutic. These studies lay the foundation for the antitumor assessment studies in years 2 and 3.

2) Specific Objectives:

There were several objectives for this project period. The first objective was to determine the biodistribution of ^{18}F -TRX in normal mouse tissues. The second objective was to determine the magnitude of ^{18}F -TRX uptake in human and mouse xenografts from subcutaneous prostate cancer cell line implants. The third objective was to determine the radiotracer uptake in a PC3 dissemination model. Lastly, the final objective was to determine the uptake of ^{18}F -TRX in a genetically engineered mouse model with prostate specific deletion of Pten.

3) Significant results or key outcomes:

Much of the data generated during this project period has been reported in a recent manuscript published in ACS Central Science (see also publications section of the progress report).

Radiosynthesis of ^{18}F -TRX. The synthesis of ^{18}F -TRX required the novel 1,2,4-trioxolane precursor reagent TRX-amine in which an amine-bearing side chain has been introduced at a bridgehead position on the adamantane ring (**Figure 1**). This reagent was synthesized in eight steps, based on the general approach described for the synthesis of artefenomel and related antimalarial trioxolanes.

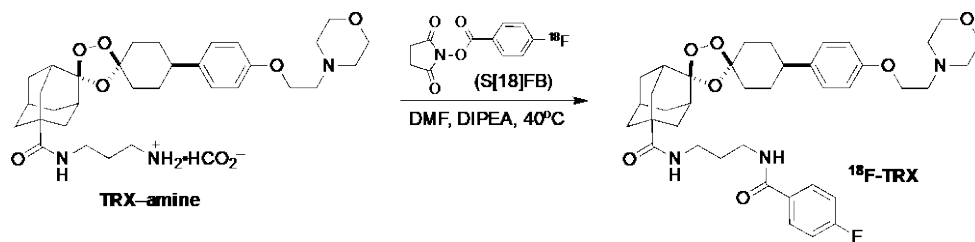


Figure 1: Radiosynthesis of ^{18}F -TRX.

The radiosynthesis of ^{18}F -TRX began with the automated preparation of ^{18}F -N-succinimidyl 4-fluorobenzoate. Using

an ELIXYS automated radiosynthesizer, ^{18}F -SFB was prepared in 75 min to a decay-corrected

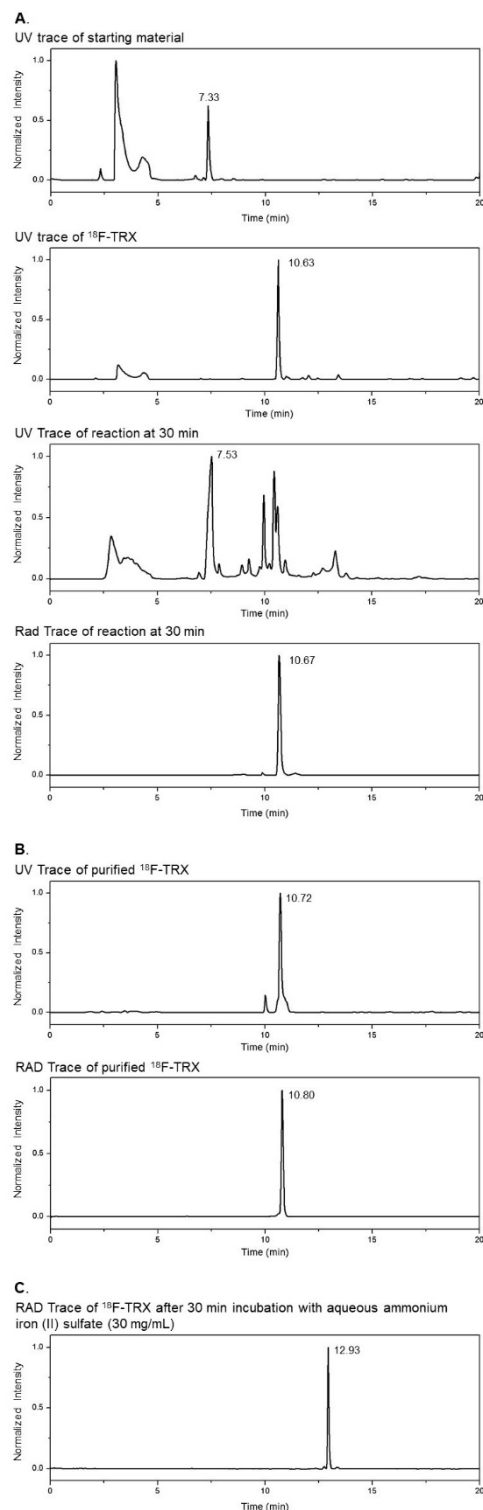


Figure 2 Synthesis and isolation of ^{18}F -TRX.

Panel A. Representative semi-preparative rad-HPLC traces showing, from top, the UV spectrum at 254 nm for TRX-amine starting material, the UV spectrum at 254 nm for the pure ^{19}F -TRX analytical standard, the UV spectrum of the complex radiochemistry reaction mixture at 40 min, and the rad spectrum of the complex radiochemistry reaction mixture at 40 min. Peaks of interest are labeled with the retention time in minutes.

Panel B. Semi-preparative rad-HPLC traces of the re-injected fraction isolated after purification. The retention time in minutes of the peak of interest representing ^{18}F -TRX is labeled.

Panel C. A rad spectrum collected 30 min after incubation of ^{18}F -TRX in aqueous ammonium Fe(II) sulfate (30 mg/mL). The peak corresponding to ^{18}F -TRX is not detected, and one new peak arises with

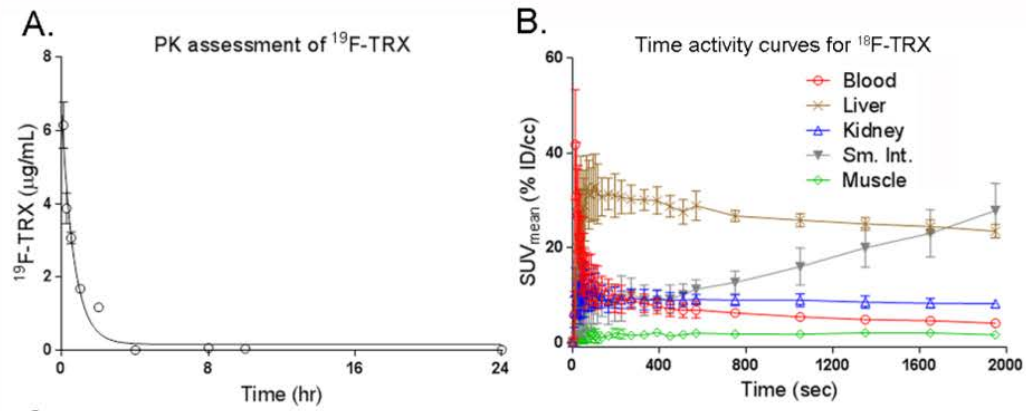
radiochemical yield of approximately 70%. For the coupling reaction, 20 mCi of ^{18}F -SFB was added to TRX-amine (5 mg of a formate salt) and 10% (v/v) DIPEA in anhydrous DMF (1 mL). The reaction was stirred at 40° C for 30 min. The reaction produced only one major radioactive peak, which co-migrated with the ^{19}F -TRX standard (**Figure 2A**). The crude reaction was purified using semi-preparative HPLC (1:10 $\text{CH}_3\text{CN}:\text{H}_2\text{O}$ to 19:1 $\text{CH}_3\text{CN}:\text{H}_2\text{O}$ over 20 min) to obtain the radiotracer ^{18}F -TRX to a decay corrected radiochemical yield of $67 \pm 7.2\%$. The purity of the compound was verified by reinjection on semi-prep HPLC (**Figure 2B**). ^{18}F -TRX was concentrated, and immediately reconstituted for additional in vitro or animal studies. The specific activity of ^{18}F -TRX was calculated to be 0.052 ± 0.02 Ci/ μmol .

^{18}F -TRX biodistribution is Fe(II) dependent in normal mouse tissues. To determine the biodistribution of ^{18}F -TRX in clinically relevant mouse models, the radiotracer was injected into immunocompetent C57Bl/6J mice and studied over time.

Region of interest analysis of a dynamic PET/CT acquisition from 0 – 60 minutes post injection revealed several enlightening trends. First, ^{18}F -TRX rapidly cleared from the mediastinal blood pool at a rate ~ 60 times faster than what we observed from a classic PK assessment of ^{19}F -TRX (**Figure 3A**). Moreover, ^{18}F -TRX rapidly accumulated in liver from 0 – 60 sec, suggesting that the radiotracer may be metabolized and cleared through this

organ (**Figure 3B** and **3C**) as is the case for artefenomel in humans.³⁰ Kidney accumulation of the radiotracer was also observed, but the uptake was significantly lower than liver. Moreover, kidney uptake plateaued within 30 sec post injection, suggesting that (as with artefenomel) renal clearance is not the dominant mechanism of clearance of radiotracer. Focal uptake in a region of the small intestine was also observed early after radiotracer injection, and the accumulation steadily increased from 400 – 3600 sec. This observation is also consistent with a model of hepatobiliary excretion. To study radiotracer distribution over a broader window of time, ex vivo biodistribution studies were conducted at 30, 60, and 90 min post injection of ¹⁸F-TRX in a separate cohort of mice (**Figure 3D**). These studies generally corroborated the PET findings, showing that ¹⁸F-TRX uptake was dominant in the liver, components of the small intestine, and the kidneys. Moreover, radiotracer uptake generally increased from 30-90 min in these tissues. Radiotracer uptake was also observed in the spleen, pancreas, stomach, large intestine, and lungs. Uptake in the brain was very low, consistent with previous observations that other TRX conjugates do not cross the blood-brain barrier.³¹

To better understand the localization of the radiotracer within regions of the small intestine, components of the GI tract were excised from a representative mouse 60 min post injection and radiotracer biodistribution was assessed with PET/CT (**Figure 3E**). This study suggested that radiotracer uptake was predominant in the duodenum and jejunum. Comparatively lower uptake was observed in the ileum, cecum and a truncated segment of the large intestine (purged manually to remove fecal matter).



C. Maximum Intensity Projections:

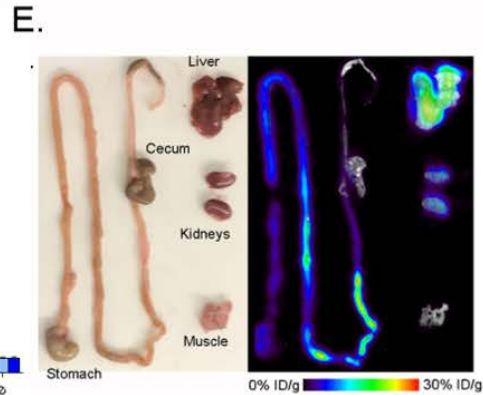
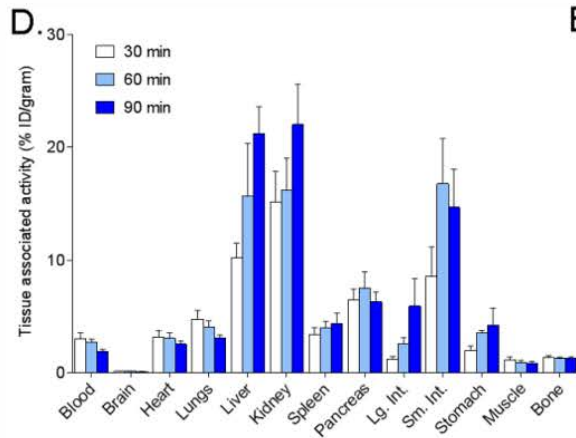
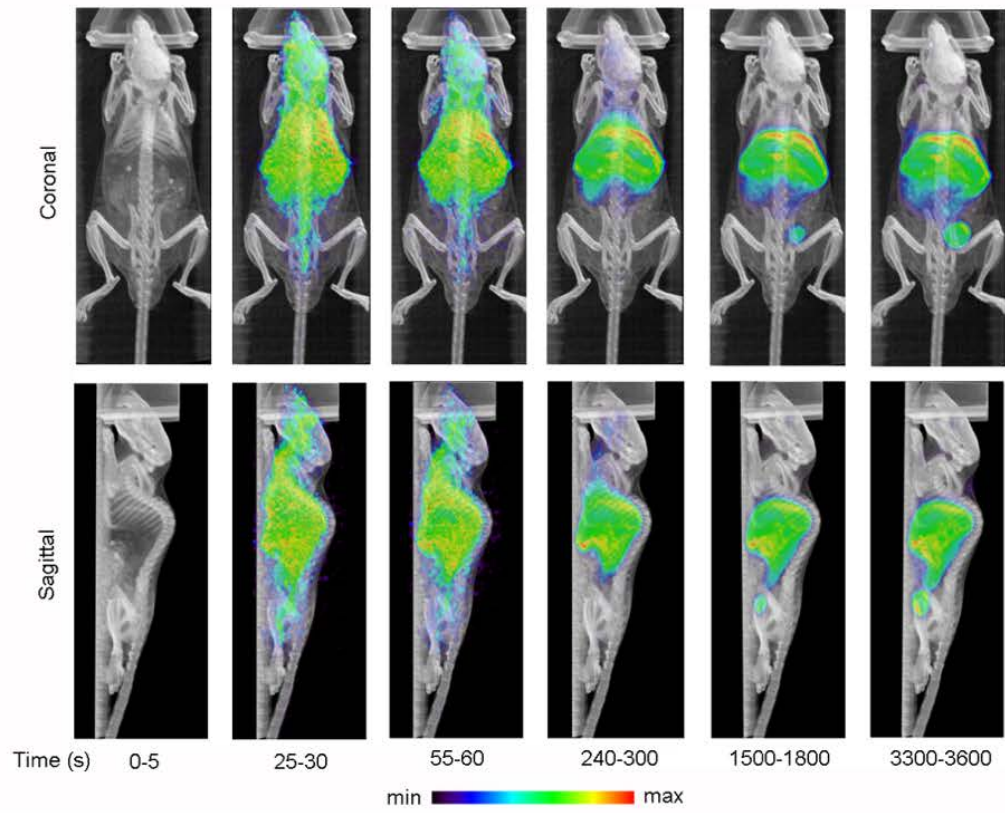


Figure 3. An in vivo assessment of the biodistribution of ^{18}F -TRX in tumor naïve immunocompetent mice. Panel A. Plasma concentration-time curve for ^{19}F -TRX administered via tail vein injection in C57Bl/6J mice revealing a plasma half-life of ~30 min. Panel B. Time activity curves derived from region of interest analysis of a 1 hour dynamic PET scan reveal radiotracer biodistribution in vivo. The radiotracer rapidly clears from the blood (red) with a calculated serum half-life of about 25 sec. The radiotracer is also sequestered within 60 sec by the liver (tan) and kidneys (blue), with no additional accumulation from 60 to 3600 sec. Liver uptake is significantly higher than what is observed in kidneys. Also, ^{18}F -TRX accumulation in the small intestine (grey) steadily increases from 0 to 3600 sec, consistent with a model of hepatobiliary clearance for the radiotracer. Little uptake is observed in the muscle (green). Panel C. Maximum intensity projections sampled serially over short time frames from the dynamic acquisition show the biodistribution of the radiotracer in normal tissues over time. A diffuse signal is observed at early time points, which gradually consolidates into the liver, kidney, and small intestine. Panel D. Biodistribution data acquired at 30, 60, and 90 min post injection of ^{18}F -TRX shows continuous accumulation of the radiotracer in many abdominal organs. The highest uptake was observed in the liver, kidneys, and small intestine. Radiotracer accumulation was low in the blood pool and muscle, as expected from the MIPs. Panel E. A PET/CT shows the biodistribution of ^{18}F -TRX in components of the gastrointestinal tract after dissection from a mouse. Prominent uptake was observed in the duodenum and jejunum, while comparatively lower radiotracer uptake was noted in the stomach, ileum, cecum, and large intestine. Liver, kidneys, and muscle are included for perspective on the upper and lower bound of radiotracer uptake in tissues.

We next tested whether ^{18}F -TRX biodistribution was impacted by exogenous treatments designed to alter tissue concentrations of ferrous iron. Twenty minutes prior to i.v. injection of ^{18}F -TRX, immunocompetent mice were treated with an i.p. bolus of PBS, ferric ammonium citrate (FAC, 20 mg/kg), desferrioxamine (50 mg/kg, DFO), deferiprone (50 mg/kg, DFP), or a mixture of FAC (20 mg/kg) pre-complexed with desferrioxamine (50 mg/kg, FAC + DFO). The use of a ferric iron source ensures that bioconversion to ferrous iron by normal cellular processes is a necessary prelude to reaction with ^{18}F -TRX. The biodistribution of the radiotracer at 60 min post injection was strikingly different between treatment arms on PET/CT (**Figure 4A**). For instance, while ^{18}F -TRX most visibly accumulated in the liver of mice treated with PBS, FAC treatment elevated uptake in the liver, small intestine, and gall bladder. Iron depleting strategies (e.g. DFO, FAC + DFO, DFP) reduced radiotracer uptake in the liver, while clearly redistributing ^{18}F -TRX to components of the small intestine. Quantitative biodistribution studies showed a statistically significant increase in ^{18}F -TRX uptake in the liver, spleen, pancreas, and duodenum of mice treated with FAC versus those treated with PBS (**Figures 4B**). Moreover, treatment with iron chelating agents significantly reduced ^{18}F -TRX uptake in virtually all tissues, with the notable exceptions of the duodenum, ileum, cecum, and large intestine in the FAC + DFO treatment arm. In summary, these data demonstrate that ^{18}F -TRX biodistribution is substantially influenced by exogenous treatments designed to modulate tissue concentrations of ferrous iron.

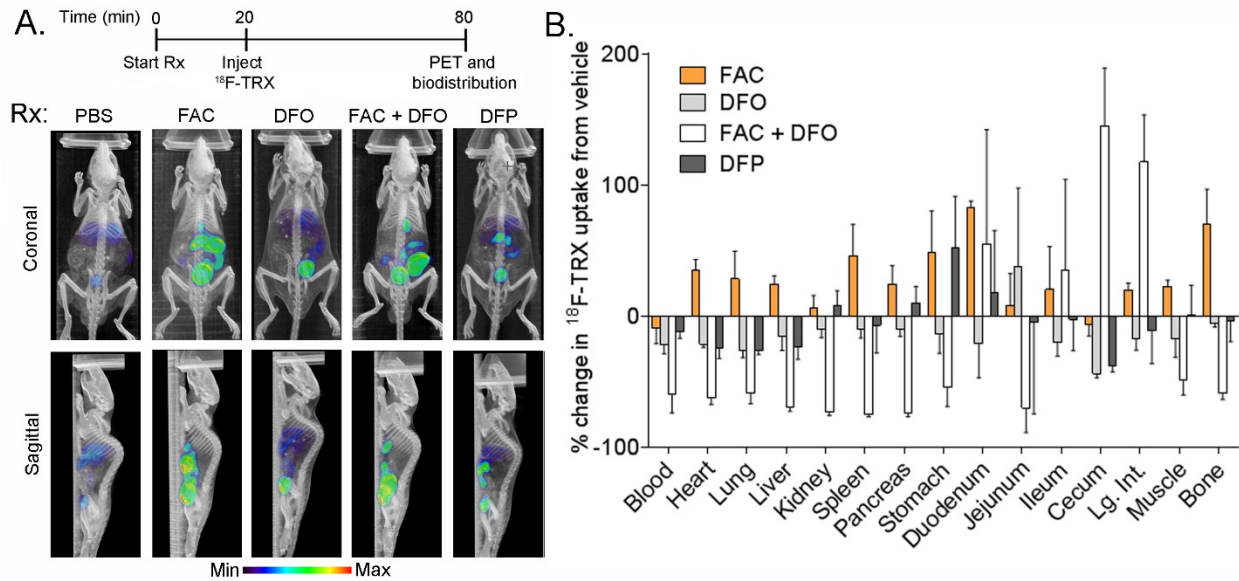


Figure 4. ¹⁸F-TRX biodistribution is substantially altered by exogenous treatments that change intracellular iron homeostasis. Panel A. (top) A timeline outlining the sequence of injections in immunocompetent C57Bl/6J mice prior to PET/CT and biodistribution studies. (bottom) Representative maximum intensity projections (MIPs) showing the biodistribution of ¹⁸F-TRX in mice from each treatment arm from 50-60 minutes post injection. Radiotracer uptake was predominantly in the liver of mice pre-treated with PBS, while pre-treatment with ferric ammonium citrate (FAC) augmented radiotracer uptake in nearly all organs, including the liver and components of the gastrointestinal tract. Pre-treatment with various iron depleting agents, including desferrioxamine (DFO), FAC complexed with DFO, and deferipone (DFP), generally reduced radiotracer uptake in organs and accelerated clearance. The MIPs, while inherently semi-quantitative, were derived from decay corrected PET data with scale bars adjusted to a range of 0% ID/g to 50% ID/g to enable gross comparison. Panel B. Biodistribution data collected at 60 min post injection show the percent changes in radiotracer uptake for selected organs in each treatment arm compared to mice receiving PBS. Relative increases in radiotracer uptake due to FAC treatment were observed in nearly all organs, while iron depleting treatments generally reduced organ uptake of the radiotracer. Treatment with FAC + DFO enhanced radiotracer uptake in components of the gastrointestinal tract, which may reflect accelerated clearance of the radiotracer.

¹⁸F-TRX detects prostate cancer tumor xenografts. We next evaluated if ¹⁸F-TRX can detect human tumors derived from cell lines previously shown to harbor sensitivity to trioxolane prodrugs. Biodistribution studies were first conducted in intact male nu/nu mice bearing subcutaneous PC3 xenografts at 30, 60, and 90 min post injection of ¹⁸F-TRX. The uptake of the radiotracer steadily increased from 30 – 90 min post injection. Radiotracer levels in the tumor significantly exceeded blood and muscle at 90 min post injection with a tumor to blood ratio of 1.97 ± 0.4 and a tumor to muscle ratio of 1.90 ± 0.3 (Figures 5A).

We further tested if ^{18}F -TRX can detect PC3 implanted in the renal capsule, as subcutaneous implants, while convenient, do not model a clinically relevant tumor microenvironment. Biodistribution studies conducted 90 min post injection of ^{18}F -TRX showed equivalent radiotracer uptake in a PC3 tumor embedded in the renal capsule compared to the extent of uptake in subcutaneous PC3 tumors (**Figure 5B**). ^{18}F -TRX uptake was also significantly higher than background (blood and muscle) in subcutaneous EKVX and U251 tumors, two models of human lung adenocarcinoma and glioblastoma, respectively (**Figure 5B**). The U251 tumor, the model with the highest ^{18}F -TRX uptake, was visually obvious on small animal PET/CT (**Figure 5C**). Ex vivo analysis of the spatial distribution of the radiotracer in U251 tumors showed that ^{18}F -TRX was well distributed through the tumor xenograft, with the regions of highest uptake appearing to have the densest cellularity on H&E (**Figure 5D**). Collectively, these data show that genetically and pathologically diverse models of human cancer harbor high avidity for ^{18}F -TRX in vivo.

We next conducted an imaging study in a genetically engineered mouse model of prostate cancer. A 10 month old Pb-Cre:Pten^{fl/fl} mouse with invasive adenocarcinoma was treated with ^{18}F -TRX, and after 90 minutes, the whole prostate was resected post mortem and imaged with PET/CT. Radiotracer uptake was visually higher in the prostate tissue compared to seminal vesicles and muscle (**Figure 5E**). Moreover, ^{18}F -TRX uptake was predominant in the prostate tissue, and not observed in the cysts that routinely develop in this disease model.

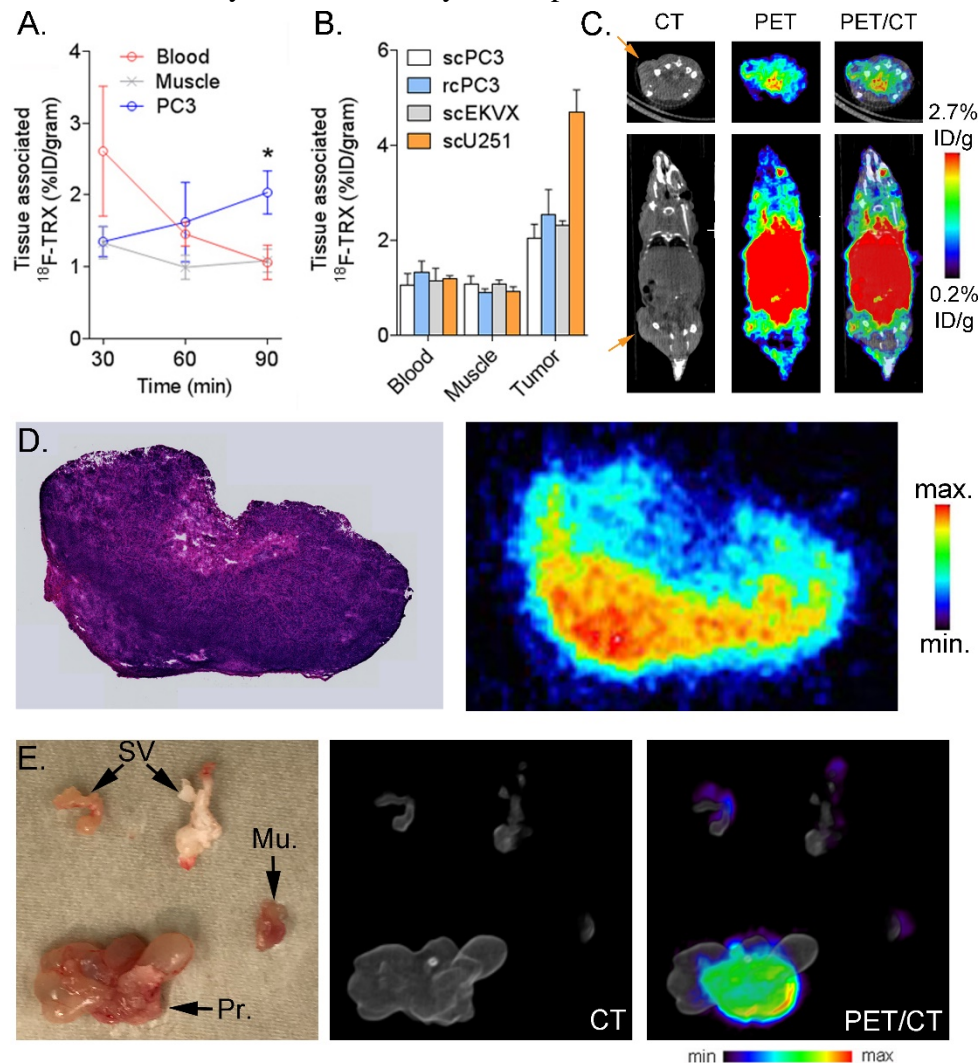


Figure 5. ^{18}F -TRX targets tumor tissue in vivo in genetically and pathologically diverse cancer models. Panel A. Biodistribution data acquired at 30, 60, and 90 min post injection of ^{18}F -TRX in male nu/nu mice with subcutaneous PC3 xenografts. The radiotracer uptake in the tumor continually increases from 30-90 min, consistent with a biochemical mechanism of action. Moreover, radiotracer uptake in the tumor exceeds the level observed in blood and muscle at 90 min post injection, two standard reference compartments for background radiotracer accumulation. The human prostate cancer model PC3 was prioritized as it was previously shown to be highly sensitive to an Fe(II)-sensitive TRX prodrug bearing a chemotherapeutic payload.³² * $P < 0.01$ compared to blood and muscle. **Figure S4** shows the biodistribution values for the entire repertoire of tissues from this animal cohort as well as the tumor to normal tissue ratios. Panel B. Biodistribution data acquired 90 min post injection of ^{18}F -TRX shows radiotracer uptake in tumor exceeding background for PC3 tumors implanted in the renal capsule (rcPC3), and subcutaneous EK VX and U251 tumors (scEK VX, scU251). **Figure S5** shows a MR image highlighting the tumor burden in renal capsule. Figure S6 shows the complete biodistribution data sets, and the tumor to normal tissue ratios. Panel C. PET/CT imaging data showing uptake of ^{18}F -TRX in tumor and normal tissues for mice bearing subcutaneous U251 tumors. The data was acquired at 90 min post injection. Panel D. H&E (left) and digital autoradiography (right) showing ^{18}F -TRX distribution within a representative section of U251 tumors. ^{18}F -TRX appears to be present in all regions of the slice, with the highest relative uptake appearing to co-localize with the area of densest cellularity on H&E. Panel E. (left) A photograph of the surgically excised whole prostate (Pr.), a piece of muscle from the hindlimb (Mu.), and the seminal vesicles (SV) of a ten month old Pb-Cre:Pten^{fl/fl} mouse with fully invasive adenocarcinoma. Cysts extending from the anterior prostate are evident by eye. (middle) A volume rendered CT image of the tissues acquired on a small animal PET/CT. (right) A volume rendered PET/CT image of ^{18}F -TRX uptake in the tissues acquired 90 min post injection of ^{18}F -TRX. The image clearly shows relatively higher accumulation of radiotracer in the diseased prostate compared to muscle or seminal vesicles. ^{18}F -TRX was excluded from the cysts, as expected.

4. Other achievements:

We have begun the synthesis of a TRX analogue functionalized with a chelator for radiolabeling with lutetium-177. We plan to conduct labeling and biodistribution studies in preparation for antitumor assessment studies. We have disclosed our findings as one peer reviewed publication and two conference abstracts (see products).

What opportunities for training and professional development has the project provided?

Nothing to report

How were the results disseminated to communities of interest?

Nothing to report

What do you plan to do during the next reporting period to accomplish the goals?

We will continue to establish the mouse prostate cancer models and conduct imaging and biodistribution experiments with ^{18}F -TRX. We will aim to report these studies in a follow-up manuscript to the first publication, which was primarily meant to establish proof-of-concept that Fe(II) can be imaged with PET in normal and a few select cancer models.

We will also begin testing the antitumor efficacy of TRX-CBI in prostate cancer animal models. To this end, the Renslo laboratory has begun synthesis of the therapeutic, and the Ruggero lab has expanded a transgenic animal colony of mice with spontaneous prostate cancer. We also have all of the cell line models required to establish the animal models.

Lastly, we have begun the synthesis of a TRX conjugate for radiolabeling with Lu-177. We anticipate beginning pilot labeling studies during this project period, and preliminary mouse biodistribution studies prior to antitumor assessment studies.

4. IMPACT:

What was the impact on the development of the principal discipline(s) of the project?

We have shown for the first time that the intracellular labile iron pool can be targeted with a translational imaging strategy (i.e. PET) that is ideal for studying the biology of metastatic castration resistant prostate cancer. Our imaging technology and data provide the first evidence that clinically relevant mouse models of prostate cancer maintain high levels of iron. While these data suggest that iron could be targeted to for imaging to improve the detection of prostate cancer disease burden—itself a major unmet clinical need—they also provide a clear scientific rationale for testing if therapies can be implemented to treat prostate cancer tumors by targeting iron. This is an entirely new approach for treating prostate cancer that is nevertheless well justified based on successful antimicrobial therapies. Lastly, our technology for imaging iron is a crucial advance for cell biology, and the scientific community is now poised to use imaging to study iron flux in normal cellular physiology, and potentially non-malignant human disorders.

What was the impact on other disciplines?

Our interest in developing new anti-cancer diagnostics and therapeutics by targeting the labile iron pool parallels other imaging and medicinal chemistry efforts targeting LIP in non-malignant disorders. Other animal imaging approaches have relied on low resolution imaging modalities like bioluminescence, and some strategies require exotic genetic engineering of mice to express reporter proteins like luciferase. Our nuclear imaging strategy is much higher resolution, absolutely rather than semi-quantitative, and does not require any special genetic manipulation of mice. In this respect, our technology is poised to sensibly complement the ongoing imaging efforts in preclinical animal models of infectious disease by groups like Dr. Chris Chang's laboratory at UC Berkeley. The therapies that we are developing could potentially be applied to non-malignant neoplastic disorders, particularly those driven by mTORC1 or RAS. These include maladies like tuberous sclerosis complex and lymphangioliomyomatosis, and RASopathies like neurofibromatosis.

What was the impact on technology transfer?

Nothing to report.

What was the impact on society beyond science and technology?

Nothing to report.

5. CHANGES/PROBLEMS:

Nothing to report

Changes in approach and reasons for change

We have de-emphasized the use of the ^{18}F -dioxolane (DXL) negative control compound during this project period. While the synthesis was straightforward and high yielding, we found that studying the biodistribution of ^{18}F -TRX after iron supplementation or withdrawal provided the necessary data to show that radiotracer accumulation in normal tissues was iron dependent. This experiment is also a better representation of naturally occurring changes in tissue concentrations of iron owing to environmental factors.

Actual or anticipated problems or delays and actions or plans to resolve them

Project period one was generally very productive, and we did not encounter many challenges. We have remaining animal imaging experiments to execute using subcutaneous models and a PC3 dissemination model. We do not anticipate any challenges in setting up these animals, nor any difficulties with conducting the imaging studies. We were slightly delayed in executing these studies as we conducted some crucial animal biodistribution studies to show that ^{18}F -TRX biodistribution is iron dependent.

Changes that had a significant impact on expenditures

Nothing to report

Significant changes in use or care of human subjects, vertebrate animals, biohazards, and/or select agents

Significant changes in use or care of human subjects

Not applicable

Significant changes in use or care of vertebrate animals

Nothing to report. This project was approved by UCSF IACUC on August 21, 2018.

Significant changes in use of biohazards and/or select agents

Nothing to report.

6. PRODUCTS:

- **Publications, conference papers, and presentations**

Journal publications.

Muir RK, Zhao N, Wei J, Wang YH, Moroz A, Huang Y, Chen YC, Sriram R, Kurhanewicz J, Ruggero D, Renslo AR, Evans MJ. Measuring Dynamic Changes in the Labile Iron Pool in Vivo with a Reactivity-Based Probe for Positron Emission Tomography. ACS Cent Sci. 2019 Apr 24; 5(4):727-736. PMID: 31041393., federal support was acknowledged

Books or other non-periodical, one-time publications. Nothing to report.

Other publications, conference papers and presentations.

Measuring dynamic changes in the labile iron pool with a reactivity-based probe for positron emission tomography. Poster abstract at the 2019 World Molecular Imaging Congress

Measuring dynamic changes in the labile iron pool with a reactivity-based probe for positron emission tomography. Poster presentation at the 2019 UCSF Radiology research symposium.

- **Website(s) or other Internet site(s)**

Nothing to report

- **Technologies or techniques**

Nothing to report

- **Inventions, patent applications, and/or licenses**

Talukdar, P., Renslo, A.R., Blank, B.R., Muir, R.K., Evans, M.J. Trioxolane agents PCT/US2018/039768, published 03/2019

- **Other Products**

Nothing to report

7. PARTICIPANTS & OTHER COLLABORATING ORGANIZATIONS

What individuals have worked on the project?

Name: Michael Evans

Role: Principal Investigator

Nearest person month worked: 1.87

Contribution to project: Dr. Evans supervised the radiochemistry and the animal imaging and biodistribution studies. He also worked with Dr. Chen to analyze and summarize the data for the manuscript submission.

Name: Zhuo Chen

Role: Post-Doc

Nearest person month worked: 10

Contribution to project: Dr. Chen was responsible for the radiochemistry and the animal PET and biodistribution studies.

Has there been a change in the active other support of the PD/PI(s) or senior/key personnel since the last reporting period?

Nothing to report.

What other organizations were involved as partners?

Nothing to report.

8. SPECIAL REPORTING REQUIREMENTS

COLLABORATIVE AWARDS: *N/A*

QUAD CHARTS: *N/A*

9. APPENDICES:*N/A*